

# Effect of Oxygen Gradients on the Activity and Microbial Community Structure of a Nitrifying, Membrane-Aerated Biofilm

Leon S. Downing, Robert Nerenberg

Department of Civil Engineering and Geological Sciences, 156 Fitzpatrick Hall,  
University of Notre Dame, Notre Dame, Indiana 46556; telephone: +1-574-631-4098;  
fax: +1-574-631-9236; e-mail: nerenberg.l@nd.edu

Received 19 March 2008; revision received 21 May 2008; accepted 2 June 2008

Published online 11 June 2008 in Wiley InterScience (www.interscience.wiley.com). DOI 10.1002/bit.22018

**ABSTRACT:** Shortcut nitrogen removal, that is, removal via formation and reduction of nitrite rather than nitrate, has been observed in membrane-aerated biofilms (MABs), but the extent, the controlling factors, and the kinetics of nitrite formation in MABs are poorly understood. We used a special MAB reactor to systematically study the effects of the dissolved oxygen (DO) concentration at the membrane surface, which is the biofilm base, on nitrification rates, extent of shortcut nitrification, and microbial community structure. The focus was on anoxic bulk liquids, which is typical in MAB used for total nitrogen (TN) removal, although aerobic bulk liquids were also studied. Nitrifying MABs were grown on a hollow-fiber membrane exposed to 3 mg N/L ammonium. The MAB intra-membrane air pressure was varied to achieve different DO concentrations at the biofilm base, and the bulk liquid was anoxic or with 2 g m<sup>-3</sup> DO. With 2.2 and 3.5 g m<sup>-3</sup> DO at the biofilm base, and with an anoxic bulk-liquid, the ammonium fluxes were 0.75 and 1.0 g N m<sup>-2</sup> day<sup>-1</sup>, respectively, and nitrite was the main oxidized nitrogen product. However, with membrane DO of 5.5 g m<sup>-3</sup>, and either zero or 2 g m<sup>-3</sup> DO in the bulk, the ammonium flux was around 1.3 g N m<sup>-2</sup> day<sup>-1</sup>, and nitrate flux increased significantly. For all experiments, the cell density of ammonium oxidizing bacteria (AOB) was relatively uniform throughout the biofilm, but the density of nitrite oxidizing bacteria (NOB) decreased with decreasing biofilm DO. Among NOB, *Nitrobacter* spp. were dominant in biofilm regions with 2 g m<sup>-3</sup> DO or greater, while *Nitrospira* spp. were dominant in regions with less than 2 g m<sup>-3</sup> DO. A biofilm model, including AOB, *Nitrobacter* spp., and *Nitrospira* spp., was developed and calibrated with the experimental results. The model predicted the greatest extent of nitrite formation (95%) and the lowest ammonium oxidation flux (0.91 g N m<sup>-2</sup> day<sup>-1</sup>) when the membrane DO was 2 g m<sup>-3</sup> and the bulk liquid was anoxic. Conversely, the model predicted the lowest extent of nitrite formation (40%) and the highest ammonium oxidation flux

(1.5 g N m<sup>-2</sup> day<sup>-1</sup>) when the membrane-DO and bulk-DO were 8 g m<sup>-3</sup> and 2 g m<sup>-3</sup>, respectively. The estimated kinetic parameters for *Nitrospira* spp., revealed a high affinity for nitrite and oxygen. This explains the dominance of *Nitrospira* spp. over *Nitrobacter* spp. in regions with low nitrite and oxygen concentrations. Our results suggest that shortcut nitrification can effectively be controlled by manipulating the DO at the membrane surface. A tradeoff is made between increased nitrite accumulation at lower DO, and higher nitrification rates at higher DO.

Biotechnol. Bioeng. 2008;xxx: xxx–xxx.

© 2008 Wiley Periodicals, Inc.

**KEYWORDS:** nitrification; shortcut; membrane-aerated biofilm reactor; membrane biofilm reactor; kinetics; *Nitrospira* spp.; *Nitrobacter* spp.

## Introduction

Total nitrogen (TN) removal from wastewater is an increasingly important treatment objective, and cost-effective TN removal methods are needed. Shortcut nitrogen removal can enhance the cost-effectiveness of any TN removal process. In shortcut nitrogen removal, ammonium is oxidized to nitrite by ammonia oxidizing bacteria (AOB) (“shortcut nitrification”), and then reduced to nitrogen gas by denitrifying bacteria (DNB) (“shortcut denitrification”). Shortcut nitrogen removal avoids formation of nitrate (van Loosdrecht and Jetten, 1998), reducing oxygen requirements by up to 25% and electron donor requirements by up to 40% (Hellinga et al., 1998).

In order to achieve shortcut nitrogen removal, nitrite oxidizing bacteria (NOB) must be inhibited. This can be achieved by selective washout of NOB at high temperatures (Hellinga et al., 1998), high free ammonia (FA) concentrations (Anthonisen et al., 1976), high pH values (Villaverde et al., 1997), or low dissolved oxygen (DO) concentrations

Correspondence to: R. Nerenberg

Contract grant sponsor: Cooperative Institute for Coastal and Estuarine Environmental Technology (CICEET)

Contract grant sponsor: National Science Foundation (NSF)

(Munich et al., 1996). Most research on shortcut nitrogen removal has focused on wastes with high  $\text{NH}_4^+:\text{COD}$  ratios and high temperatures, such as digester centrate, where NOB-inhibiting conditions (e.g., high temperature, high FA) are provided. For municipal wastewater treatment, the most feasible inhibition method may be low DO (Yang et al., 2007). Since AOB have higher yields and a lower half-saturation coefficient for oxygen than NOB (Schramm et al., 1998), they typically outcompete NOB at low DO concentrations (Munich et al., 1996; Slikers et al., 2005). Unfortunately, it is difficult to maintain the correct DO for shortcut nitrification and denitrification without inhibiting nitrification or denitrification, as seen in the simultaneous nitrification denitrification (SND) process (Pochana and Keller, 1999).

An improved approach for DO control to achieve shortcut nitrogen removal is the use of membrane-aerated biofilms (MABs) (Syron and Casey, 2008). MABs use air or oxygen-filled membranes to transfer oxygen to biofilms naturally forming on the membrane surface (Semmens et al., 2003). Unlike conventional biofilms, where electron donors and oxygen enter the biofilm from the bulk liquid, MABs supply oxygen from the attachment surface (Timberlake et al., 1988). This makes MABs ideal for retaining nitrifying bacteria, as they provide oxygen deep in the biofilm, where nitrifiers are protected from detachment, predation, and competition from heterotrophic bacteria (Cole et al., 2004; LaPara et al., 2006). The DO at the base of an MAB can be set by adjusting in the intra-membrane air pressure, providing DO regions favorable to AOB but not to NOB (Terada et al., 2006). When the outer portions of the MAB are anoxic, denitrification can take place concurrently with nitrification (Satoh et al., 2000).

Shortcut nitrogen removal has been verified in several MAB studies. Downing and Nerenberg (2007, 2008) studied a new MAB process, called the hybrid membrane biofilm process (HMBP), where nitrification was carried out in an MAB and denitrification was carried out by suspended bacteria in the anoxic bulk liquid. When the DO at the membrane–biofilm interface was  $3.5 \text{ g m}^{-3}$  in the HMBP, the nitrite formation rate was at least three to four times greater than that of nitrate (Downing and Nerenberg, 2008). Schramm et al. (2000) studied a nitrifying MAB in an anoxic bulk liquid, and found that, with a DO concentration of  $6.4 \text{ g m}^{-3}$  at the membrane surface, the nitrite production rates were twice that of nitrate. Other MAB reactors (MABRs) achieving TN removal had low levels of nitrate in the biofilm (Hibiya et al., 2003), and an oxygen mass balance in another study indicated that most oxygen transferred to an MABR was used for ammonia oxidation, with little oxygen remaining for nitrite oxidation (Terada et al., 2003). Terada et al. (2006) showed that nitrification rates in an MAB could be controlled by manipulating the intra-membrane air supply pressure, which affects the oxygen concentration at the membrane–biofilm interface, and found nitrite accumulation in the bulk. However, oxygen concentrations within the biofilm were not examined, nor

was the relationship between oxygen concentrations and the MAB's microbial community structure. It was also unclear if the oxygen concentration or ammonium loading was the controlling parameter for shortcut nitrification in the study.

*Nitrobacter* spp. and *Nitrospira* spp. are commonly found in nitrifying activated sludge processes, with *Nitrobacter* spp. historically assumed to be the dominant NOB (Siripong and Rittmann, 2007). However, recent research suggests that *Nitrospira* spp. are the dominant NOB in wastewater treatment systems (Burrell et al., 1999; Harms et al., 2003; Juretschko et al., 1998). It has been suggested that *Nitrobacter* spp. are r-strategists, whereas *Nitrospira* spp. are K-strategists for nitrite (Blackburne et al., 2007b; Nogueira and Melo, 2006). In an MAB with an anoxic bulk liquid, *Nitrospira* spp. were dominant in the low DO portions of the biofilm, while *Nitrobacter* spp. dominated the high DO portions, suggesting the oxygen concentration also plays a critical role in the competition of *Nitrobacter* spp. and *Nitrospira* spp. (Schramm et al., 2000). The selection of *Nitrospira* spp. and *Nitrobacter* spp. is important in nitrification processes because *Nitrobacter* spp. have significantly higher nitrite oxidation rates than *Nitrospira* spp. (Schramm et al., 1999), which can impact the amount of nitrite accumulation occurring in the system.

While MABs can achieve shortcut nitrogen removal, it is not clear what DO concentration at the membrane surface is required to achieve the desired oxygen gradients in the biofilm to maximize the extent of shortcut nitrification. Also, while low DO should increase nitrite accumulation, it may also reduce ammonium oxidation rates by AOB, and the tradeoff between obtaining a high degree of shortcut nitrification and obtaining high nitrification rates is unknown. This research uses fluorescence in situ hybridization (FISH) and microsensors to systematically explore the effects of DO on the extent of shortcut nitrification in an MAB, nitrification kinetics in an MAB, and the abundance of nitrifying bacteria in a nitrifying MAB. Biofilm modeling was utilized to determine kinetic parameters for *Nitrobacter* and *Nitrospira* spp., and infer the effects of oxygen gradients on nitrification rates for a wider range of DO gradients.

## Materials and Methods

### Reactor Configuration

A column reactor with a single hollow-fiber membrane was used to simulate an HMBP or MABR biofilm achieving TN removal. The membranes used were a composite, microporous polyethylene with a dense, polyurethane core (HFM200TL, Mitsubishi Rayon, Japan). Nitrification performance was studied as a function of intra-membrane air supply pressure. A recycle reservoir was continuously purged with nitrogen gas to maintain an anoxic bulk liquid. The reactor consisted of a 6-mm inside diameter glass tube, 20 cm in length, with three, 3-mm diameter ports along the length of the column (Fig. 1). Reactor components

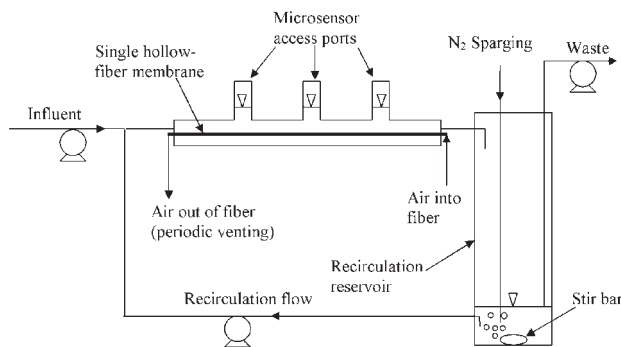


**Figure 1.** Schematic of column reactor.

are described in Table I. The ports were used for microsensor measurements of DO, ammonium, nitrite, and nitrate in the biofilm. A magnetic stir bar kept the reservoir well-mixed with a high shear velocity, minimizing biofilm growth on the glass surface. The total liquid volume in the reactor was 56 mL. A volume of 40 mL was maintained in the recirculation reservoir by an effluent pump. The influent flow rate was 2 mL/min, providing a hydraulic retention time (HRT) of 28 min. The short HRT prevented the accumulation of suspended nitrifying bacteria, and anoxic bulk liquid conditions during most of the experimental conditions prevented nitrifying biofilms from growing on glass surfaces. The reactor temperature was 22°C. The recirculation flow rate was 50 cm<sup>3</sup> min<sup>-1</sup>, resulting in a fluid velocity of 30 cm s<sup>-1</sup> and a Reynolds number of 680 inside the column. The hollow-fiber membrane was normally operated in dead end mode, but the fiber was vented on a daily basis to prevent accumulation of water condensate.

### Testing Conditions

Four intra-membrane supply pressures were tested in separate column reactors. Each column reactor was inoculated with activated sludge from the Plattville, WI municipal wastewater treatment plant, which was achieving nitrification to nitrate when the sludge was collected. The influent ammonium concentration was 3 g N m<sup>-3</sup>, a typical value for an HMBP, which is a completely mixed system (Downing and Nerenberg, 2008). The loading rate was 33 g N m<sup>-2</sup> day<sup>-1</sup>, much higher than the typical 1 g N m<sup>-2</sup> day<sup>-1</sup> removal rates for MABs (Downing and Nerenberg, 2007). The high loading rate resulted in little ammonium removal within the reactor, keeping the

**Table I.** Column reactor components.

Component	Inside diameter	Length	Volume	Surface area
Glass tube	6 mm	40 cm	5 mL	—
Rubber tubing	6 mm	10 cm	1.25 mL	—
Reservoir	—	—	50 mL	—
Membrane	280 μm	18 cm	—	2.7 × 10 <sup>-3</sup> m <sup>2</sup>

ammonium concentration close to the influent value. Also, the low HRT kept bulk-liquid nitrite and nitrate concentrations at low levels, as would be found in an HMBP with denitrification in the bulk liquid (Downing and Nerenberg, 2007), or an MABR with denitrification in the outer biofilm layer (Hibiya et al., 2003; Semmens et al., 2003; Walter et al., 2005).

Four DO gradients were studied. Experiments 1, 2, and 3 had anoxic bulk liquid and intra-membrane supply pressures of 14, 35, and 70 kPa, respectively. In Experiment 4, the bulk liquid DO was 2 g m<sup>-3</sup> and the intra-membrane supply pressure as 70 kPa. Each test was run for 56 days, with microsensor measurements taken at days 42 and 56, and FISH analyses run on biofilm samples from day 56.

### Analytical Methods

Ammonia (NH<sub>3</sub>-N) concentrations were monitored in the bulk liquid using the salicylate method (Hach, Loveland, CO). A glass electrode pH meter was used to monitor pH. Nitrate (NO<sub>3</sub><sup>-</sup>-N) and nitrite (NO<sub>2</sub><sup>-</sup>-N) were analyzed by ion chromatography (IC2500 with AS11/AG11 column, Dionex Corp., Sunnyvale, CA.).

### Activity Measurements

Clark-type oxygen microsensors (Revsbech and Jorgensen, 1986) with a tip diameter of 10 μm were used to measure DO concentrations in the biofilms (Ox10, Unisense A/S, Aarhus, Denmark). Liquid ion exchange (LIX) microsensors were constructed to measure ammonium, nitrate, and nitrite concentrations in the biofilm. LIX construction was completed as previously described (Geiseke and De Beer, 2004). Nitrate (De Beer and Sweerts, 1989) and ammonium (De Beer and van den Heuvel, 1988) microsensors were constructed with a tip diameter of 3–5 μm, and the nitrite electrodes had a tip diameter of 10–15 μm (De Beer et al., 1997). All measurements were taken at spatial intervals of 20 μm through the biofilm. The sensors were moved through the biofilm with a micro-manipulator (Model MM33-2, Unisense A/S).

Microprofile measurements were made at each of the three sampling ports in the reactor on days 42 and 56. Three to five microprofiles were taken for each port. The biofilm thickness was relatively consistent along membrane length for a given experiment. A total of 9–15 sets of profiles were analyzed for each reactor on each sampling date.

Microbial flux into the biofilm was calculated to assess the nitrification rate as well as the nitrite and nitrate production rates (Geiseke and De Beer, 2004). Flux,  $J$ , between two points can be calculated using Fick's first law:

$$J_{ab} = -D_{\text{eff}} \frac{C_a - C_b}{X_a - X_b} \quad (1)$$

The flux required for rate calculations is the flux through the diffusion boundary layer. The thickness of the diffusion boundary layer,  $\delta_b$ , replaces the  $X_a - X_b$  term in

Equation (1). The diffusion boundary layer thickness was calculated as previously described (Downing and Nerenberg, 2008).

### Fluorescence In Situ Hybridization

After microsensor measurements were completed on day 56, each membrane was removed from the respective reactor and fixed in freshly prepared paraformaldehyde (4% in phosphate buffer solution (PBS)) at 4°C for 1 h and washed in PBS. Membrane bound biofilms were embedded in OCT compound (Tissue Teck, Elkhart, Indiana) and sectioned with a cryostat (Leica CM1100) at -20°C (Schramm et al., 2000). Each section was 5- $\mu\text{m}$  thick. Sections were placed on a six-welled slide (Erie Scientific, Portsmouth, NH) and dehydrated using a series of ethanol baths at 50%, 80%, and 100%, followed by drying in a 46°C oven for 1 h.

Four FISH probes were implemented: Nso190, which targets the majority of AOB (Mobarry et al., 1996); NIT3, which targets *Nitrobacter* spp. (Wagner et al., 1996); NSR1156, which targets *Nitrospira* spp. (Schramm et al., 1998); and EUB338, which targets general bacteria (Amann et al., 1990). Probes, hybridization conditions, and washing conditions are as described previously (Amann et al., 1990; Mobarry et al., 1996; Schramm et al., 1998; Wagner et al., 1996). Oligonucleotides were synthesized and fluorescently labeled with fluorochromes Cy3, Cy5, or FITC by Operon Biotechnologies, Inc. (Huntsville, AL).

All hybridizations were completed at 46°C for 90 min in a hybridization buffer containing 0.9 M NaCl, formamide at the percentage previously indicated (Amann et al., 1990; Mobarry et al., 1996; Schramm et al., 1998; Wagner et al., 1996), 20-mM Tris-HCl (pH 7.4), and 0.01% SDS (Manz et al., 1992). The probe concentration was 5 ng/ $\mu\text{L}$ . Hybridization was followed by a stringent washing step at 48°C for 10 min in washing buffer containing 20 mM Tris-HCl (pH 7.4), NaCl at the concentration previously indicated (Amann et al., 1990; Mobarry et al., 1996; Schramm et al., 1998; Wagner et al., 1996), and 0.01% SDS. Washing buffer was removed by rinsing the slides with distilled water. The slides were air dried in the dark, and stained with 4,6-diamidino-2-phenylindole (DAPI, 1 ng/ $\mu\text{L}$ ) for 2 min in the dark on ice, and rinsed again with distilled water. The slides were then mounted in an antifadent in phosphate buffered saline (Citifluor AF100, Citifluor, Ltd., London, UK) in an aqueous solution of polyvinyl alcohol (CFPVOH, Citifluor, Ltd.) to avoid bleaching. Images were examined with an epifluorescence microscope (Nikon Eclipse 90i).

Quantification was accomplished using MetaMorph software (Molecular Devices, Sunnyvale, CA). The area of a single, dispersed cell hybridized with each of the probes was first determined. This area was then assigned as a single cell. Area of cell clusters in the biofilm were then assigned cell counts via the automated cell-count function in MetaMorph. A grid of 10  $\mu\text{m}$   $\times$  10  $\mu\text{m}$  squares was applied to each image, and cell counts in each grid square were

made. These grids were then assigned distances from the membrane surface. Thresholding was completed manually and verified with manual cell counts of dispersed cells. A total of 10 images were analyzed for each probe at each condition.

### Modeling

A biofilm model was developed using the AQUASIM 2.0 computer program (Wanner and Reichert 1996) to predict MAB performance under a wide range of intra-membrane supply pressures. The kinetics of AOB genera have been well documented, and there are accepted values (Kindaichi et al., 2006; Prosser 1989; Wiesmann 1997). However, ranges of kinetic parameters for *Nitrobacter* spp. have been reported in the literature (Laanbroek and Gerards 1993; Laanbroek et al., 1994; Schramm et al., 1999), and only a few studies have examined *Nitrospira* spp. kinetics (Kim and Kim 2006; Kindaichi et al., 2006; Schramm et al., 1999). Recent studies have improved estimates of half saturation coefficient for oxygen ( $K_o$ ) and nitrite ( $K_s$ ) for *Nitrobacter* spp. and *Nitrospira* spp. (Blackburne et al., 2007a,b), and estimated the in situ maximum growth rate ( $\hat{\mu}$ ) for *Nitrospira* spp. grown in a biofilm (Kindaichi et al., 2006).

The model was similar to past MAB models (Shanahan and Semmens, 2004), but was extended to include three microbial populations: AOB, *Nitrobacter* spp. and *Nitrospira* spp. The kinetic parameters are shown in Table II. AOB were modeled with kinetic parameters for *Nitrosomonas eutropha*, as previous studies showed this lineage to be dominant in nitrifying MABs (Schramm et al., 2000). A detailed description of the stoichiometry and processes incorporated in the model are shown in Appendix A. Rather than model gas transfer via the hollow-fiber membrane, the DO at the membrane-biofilm interface was fixed as a model input parameter. The DO concentration at the membrane-biofilm interface was taken from experimental results. The biofilm density was assumed to be constant through the biofilm. Biofilm density has been shown to vary with depth in an MAB containing both nitrifiers and heterotrophs (Shanahan et al., 2005); however, density in a mainly nitrifying MAB was shown to be relatively consistent through the use of FISH (Downing and Nerenberg, 2008), and therefore the density was assumed to be constant.

The kinetic parameters for *Nitrobacter* spp. and *Nitrospira* spp. were fit to the experimental data for the three intra-membrane conditions, using the ranges of values provided in Table II as maximum and minimum possible values. The error was minimized using relative least-squares minimization to determine the set of kinetic parameters that best fit the experimental data.

Sensitivity analysis of the  $K_o$ ,  $K_s$ , and  $\hat{\mu}$  values for both *Nitrobacter* spp. and *Nitrospira* spp. was completed by varying each parameter by 10%, while the remaining parameters remained constant. The percent change in the nitrite flux, nitrate flux, and *Nitrobacter* spp. and *Nitrospira*

**Table II.** Kinetic parameters used in the Aquasim model.

Variable	Description	Value <sup>a</sup>	References
<i>AOB (Nitrosomonas eutropha)</i>			
$\hat{\mu}_{AOB}$	Maximum specific growth rate for AOB	0.48 day <sup>-1</sup>	Adapted from Prosser (1989)
$Y_{AOB}$	Yield for AOB	0.3 g X g N <sup>-1</sup>	Shanahan and Semmens (2004)
$q_{max,AOB}$	Maximum substrate utilization rate for AOB	1.6 g N g X <sup>-1</sup> day <sup>-1</sup>	Adapted from Prosser (1989)
$b_{AOB}$	Decay coefficient for NOB	0.13 day <sup>-1</sup>	Terada et al. (2006)
$K_{s,AOB}$	Half saturation coefficient for ammonium	0.9 g N m <sup>-3</sup>	Shanahan and Semmens (2004)
$K_{o,AOB}$	Half saturation coefficient for oxygen	0.24 g m <sup>-3</sup>	Shanahan and Semmens (2004)
<i>Nitrobacter spp.</i>			
$\hat{\mu}_{Nit}$	Maximum specific growth rate for <i>Nitrobacter</i> spp.	0.3–0.34 day <sup>-1</sup>	Adapted from Prosser (1989)
$Y_{nit}$	Yield for <i>Nitrobacter</i> spp.	0.08 g X g N <sup>-1</sup>	Blackburne et al. (2007a)
$q_{max,Nit}$	Maximum substrate utilization rate for <i>Nitrobacter</i> spp.	3.76–4.2 g N g X <sup>-1</sup> day <sup>-1</sup>	Adapted from Prosser (1989)
$b_{Nit}$	Decay coefficient for <i>Nitrobacter</i> spp.	0.1 day <sup>-1</sup>	Terada et al. (2006)
$K_{s-Nit}$	Half saturation coefficient for nitrite	0.36–0.39 g N m <sup>-3</sup>	Blackburne et al. (2007b)
$K_{o-Nit}$	Half saturation coefficient for oxygen	0.35–0.51 g m <sup>-3</sup>	Blackburne et al. (2007b)
<i>Nitrospira spp.</i>			
$\hat{\mu}_{Nsr}$	Maximum specific growth rate for <i>Nitrospira</i> spp.	0.264–0.33 day <sup>-1</sup>	Adapted from Kindaichi et al. (2006)
$Y_{Nsr}$	Yield for <i>Nitrospira</i> spp.	0.15 g X g N <sup>-1</sup>	Blackburne et al. (2007a)
$q_{max,Nsr}$	Maximum substrate utilization rate for <i>Nitrospira</i> spp.	1.76–2.2 g N g X <sup>-1</sup> day <sup>-1</sup>	Adapted from Prosser (1989)
$b_{Nsr}$	Decay coefficient for <i>Nitrospira</i> spp.	0.1 day <sup>-1</sup>	Terada et al. (2006)
$K_{s-Nsr}$	Half saturation coefficient for nitrite	0.27–0.33 g N m <sup>-3</sup>	Blackburne et al. (2007b)
$K_{o-Nsr}$	Half saturation coefficient for oxygen	0.4–0.68 g m <sup>-3</sup>	Blackburne et al. (2007b)

<sup>a</sup>X is biomass expressed as dry weight.

spp. population fractions was used to assess the sensitivity of the model to the kinetic parameters. The sensitivity analysis was performed for the membrane surface DO of 5 g m<sup>-3</sup>. This condition was chosen because it resulted in similar nitrite and nitrate fluxes, and similar amounts of *Nitrobacter* spp. and *Nitrospira* spp.

After determining best-fit kinetic parameters for NOB, the model was used to assess a broader range of membrane surface DO concentrations and the impact of bulk liquid DO concentration on shortcut nitrification.

## RESULTS

### Experimental Results

#### Oxygen Gradients

Due to the decreased oxygen transfer at lower intra-membrane pressures (Terada et al., 2006), the measured DO concentration at the membrane surface can be less than predicted by Henry's Law. Table III compares the measured oxygen concentrations to those calculated from Henry's Law, assuming a Henry's Constant ( $K_H$ ) for oxygen of

41.6 mg L<sup>-1</sup> atm<sup>-1</sup> (Manahan, 1993), and compressed air as the supply gas. Table III also provides the measured biofilm thicknesses, and the percent of biofilm thickness exposed to DO concentrations below 2 g m<sup>-3</sup>. Decreased intra-membrane pressure resulted in decreased DO concentrations at the membrane surface, effectively reducing the oxygen gradient in the MAB.

#### Nitrification Rates and Nitrite Accumulation

Profiles for DO, ammonium, nitrite, and nitrate were determined using microsensors (Fig. 2). Since the values for days 42 and 56 were very similar, the biofilm was assumed to be at steady state by day 42, and the data from both dates were combined in Figure 2. Each plot is in terms of normalized biofilm thickness, as biofilm thickness varied among sampling locations and dates by 10–20  $\mu$ m.

In Experiment 4, where the bulk liquid DO was approximately 2 g m<sup>-3</sup>, a significant amount of biofilm was observed on the walls of the column reactor. This resulted in reduced bulk liquid ammonium concentrations, but the flux of ammonium into the biofilm should not have been impacted, because the ammonium concentrations were still above their rate-limiting values. Wall growth was only

**Table III.** Oxygen concentration at the membrane–biofilm interface and biofilm thickness.

Experiment	Intra-membrane Pressure (gauge) (kPa)	Calculated oxygen concentration at membrane <sup>a</sup> (g m <sup>-3</sup> )	Measured oxygen concentration at membrane (g m <sup>-3</sup> )	Biofilm thickness ( $\mu$ m)	Biofilm with DO below 2 g m <sup>-3</sup> (%)
1	14	9.5	2.2 $\pm$ 0.2	80	85
2	35	11.2	3.5 $\pm$ 0.2	100	65
3	70	14.1	5.5 $\pm$ 0.6	100	40
4	70 (aerobic bulk)	14.1	5.5 $\pm$ 0.4	120	0

<sup>a</sup>Equilibrium concentration at membrane–biofilm interface determined based on Henry's constant ( $K_H$ ) and air pressure supplied to membrane lumen.

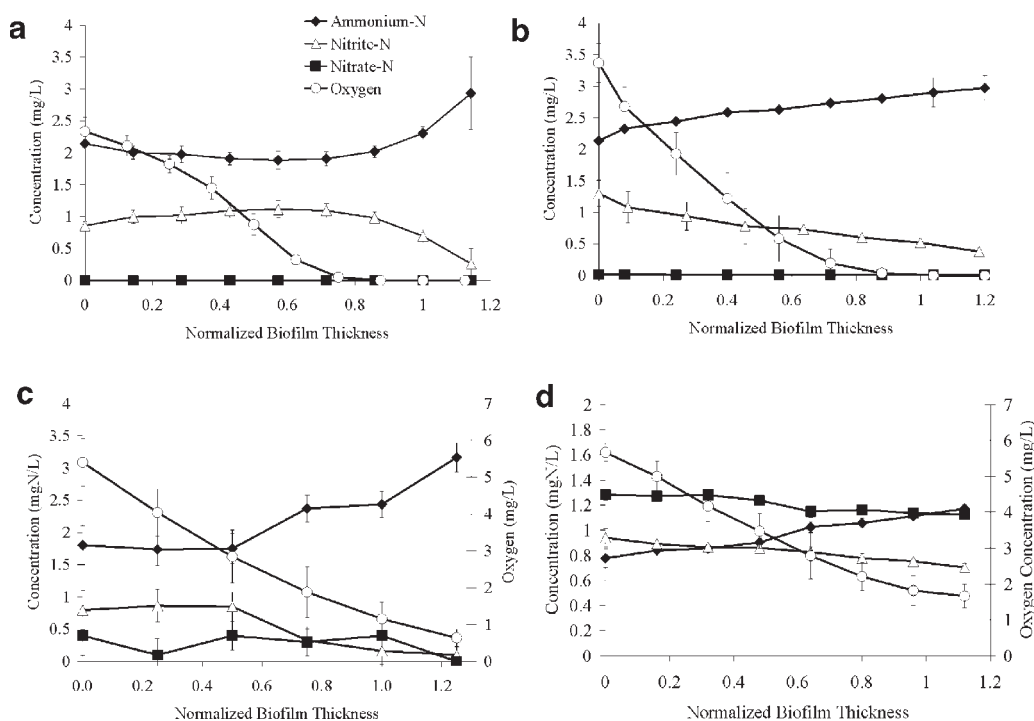


**Figure 2.** Microsensor profiles for operating pressures of (a) Experiment 1 (14 kPa), (b) Experiment 2 (35 kPa), (c) Experiment 3 (70 kPa), and (d) Experiment 4 (70 kPa with an aerobic bulk liquid). Note that the oxygen profile is on a secondary axis in (c) and (d) and the nitrogen axis has a different scale in (d) than the remaining figures. The abscissa is normalized biofilm thickness relative to the total thickness, with zero representing the base of the biofilm and 1.0 the outer edge of the biofilm.

observed in Experiment 4. The bulk liquid DO was below  $1 \text{ g m}^{-3}$  in Experiment 3, and it was anoxic in the remaining experiments, which effectively limited wall growth.

The flux of ammonium, nitrite, and nitrate were calculated based on the concentration difference between the biofilm surface and the bulk liquid and the thickness of the liquid diffusion layer. Flux results are summarized in Figure 3. The liquid diffusion layer thickness was approximately the same between each experiment for each compound, with diffusion layer thicknesses of approximately 7, 6, and  $9 \mu\text{m}$  for ammonium, nitrite, and nitrate, respectively. The ammonium flux rate matched the sum of the nitrite and nitrate flux rates within 5%. The ammonium flux decreased with each decrease in intra-membrane operating pressure, most likely due to increasing oxygen limitation in the biofilm.

Nitrite accumulation was found in each experiment, with an increasing fraction of the oxidized nitrogen accounted for by the nitrite flux with decreasing intra-membrane supply pressure. Full nitrite accumulation was achieved under an operating pressures of 14 kPa, which resulted in oxygen concentration of less than  $2 \text{ g m}^{-3}$  in over 85% of the biofilm.

### Abundance of Nitrifying Bacteria

Quantification of the distribution of AOB and NOB within the biofilm was performed for each experiment using FISH. For all experiments, the AOB density was similar throughout

the biofilm, with an average density of  $200 \times 10^9 \text{ cells cm}^{-3}$ . However, the total NOB density decreased sharply with distance from the membrane surface. Also, the maximum NOB density, which occurred at the membrane–biofilm interface, decreased with decreasing intra-membrane pressures.

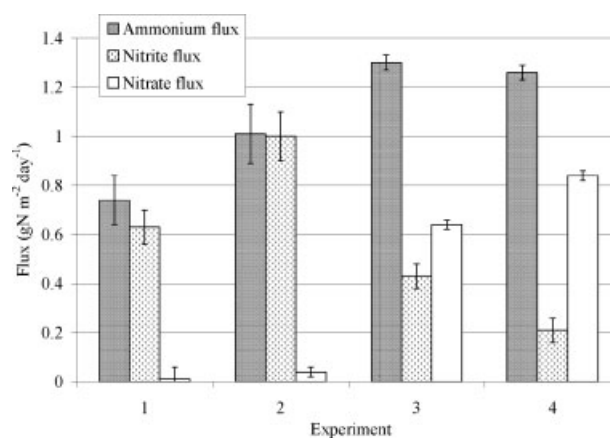


**Figure 3.** Fluxes of ammonium, nitrite, and nitrate under varying intra-membrane operating pressures. Ammonium fluxes are into the biofilm, while nitrate and nitrite are out of the biofilm. Experiment 1 had 14 kPa intra-membrane air supply pressure; Experiment 2 had 35 kPa; Experiment 3 had 70 kPa; and Experiment 4 had 70 kPa, with an aerobic bulk liquid.

No nitrate formation was detected at the lower intra-membrane operating pressures (Experiments 1 and 2), where the NOB density was less than approximately 10% of that of AOB density. When the NOB population was subdivided into *Nitrobacter* spp. and *Nitrospira* spp., a shift in the dominant species was revealed (Fig. 4a and b). At an intra-membrane pressure of 70 kPa, *Nitrobacter* spp. was the dominant NOB at the membrane surface, with a density of approximately  $18 \times 10^9$  cells  $\text{cm}^{-3}$ , as compared to a density of  $11 \times 10^9$  cells  $\text{cm}^{-3}$  for *Nitrospira* spp. The *Nitrospira* spp. density at the membrane surface remained approximately the same for each oxygen condition, but the *Nitrobacter* spp. density decreased to  $8 \times 10^9$  cells  $\text{cm}^{-3}$  and  $2 \times 10^9$  cells  $\text{cm}^{-3}$  for operating pressures of 35 and 14 kPa, respectively.

A similar population shift was observed in the biofilm 30–60  $\mu\text{m}$  from the membrane. At an intra-membrane pressure of 70 kPa, the NOB population was approximately 50% *Nitrobacter* spp. and 50% *Nitrospira* spp. At 35 kPa, the concentration of *Nitrospira* spp. was around twice that of *Nitrobacter* spp., and no *Nitrobacter* spp. were detected at a distance from the membrane greater than 30  $\mu\text{m}$  at 14 kPa, where *Nitrospira* spp. were present at approximately the same density as at 35 kPa. Very few NOB were detected at distance greater than 60  $\mu\text{m}$  from the membrane.

In Figure 4, standard deviation for each bar ( $n=10$  images) ranged from 30% to 40% for the densities of NOB. This large error was associated with the clustering of NOB within the biofilm. *Nitrospira* spp. and *Nitrobacter* spp. were present in clusters through the biofilm, and therefore portions of the biofilm effectively had a zero density of NOB, while others had elevated densities.

## Modeling Results

### Parameter Fitting

The model was calibrated with the experimental data to determine the applicable kinetic parameters. The best fit

kinetic parameters for *Nitrobacter* spp. and *Nitrospira* spp. are shown in Table IV. The  $K_o$  for *Nitrobacter* spp. was at the low end of the values reported by Blackburne et al. (2007b), and the  $K_o$  for *Nitrospira* spp. was at the high end of the values reported by Blackburne et al. (2007b). The maximum specific growth rates,  $\hat{\mu}$ , for both *Nitrobacter* spp. and *Nitrospira* spp. were within the range of maximum specific growth rates for NOB in a biofilm (Kindaichi et al., 2006). A comparison of the model and experimental fluxes for ammonium, nitrite, and nitrate is shown in Table V.

The model indicated that the fluxes and ecology were highly sensitive to  $\mu$  for both *Nitrobacter* spp. and *Nitrospira* spp. The fluxes had low sensitivity to  $K_o$  and  $K_s$ , but the ecology was sensitive to these values. See Appendix A for detailed results of the sensitivity analysis. A wide range of  $\hat{\mu}$  values have been reported for *Nitrobacter* spp. and *Nitrospira* spp. (Ehrich et al., 1995; Kindaichi et al., 2006; Prosser 1989), and the in situ  $\hat{\mu}$  for *Nitrospira* spp. in a biofilm has been shown to vary depending on the growth state of the biofilm (Kindaichi et al., 2006). Given the high sensitivity to  $\hat{\mu}$ , and its potential variability, verification of the  $\hat{\mu}$  value when modeling other experimental systems may be necessary. The  $K$  values estimated by Blackburne et al. (2007a,b) adequately predicted our observed shifts from *Nitrobacter* spp. to *Nitrospira* spp. with decreasing oxygen and nitrite concentrations.

### Impact of Oxygen on Ammonium and Nitrite Fluxes

Using the kinetic parameters shown in Table II, the biofilm model was used to determine fluxes of nitrite, nitrate, and ammonium for various membrane-surface DO concentrations (Fig. 5), and for various combinations of DO at the membrane surface and DO in the bulk liquid (Table VI). With an anoxic bulk liquid, ammonium oxidation fluxes increased with increasing DO concentrations at the membrane surface, with a sharp increase from 1 to 2  $\text{g m}^{-3}$  DO and a more linear increase from 2 to 8  $\text{g m}^{-3}$  (Fig. 5). Consistent with the experimental results,

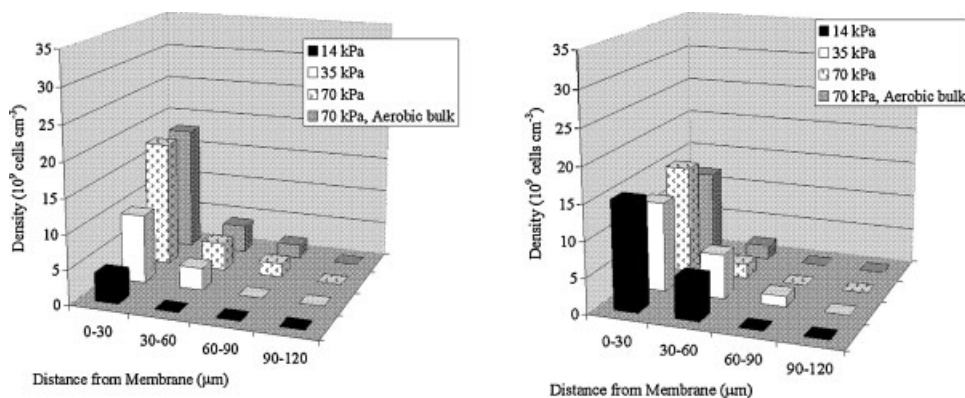


**Figure 4.** a: *Nitrobacter* spp. and (b) *Nitrospira* spp. densities in the biofilm at varying intra-membrane pressures. Error bars were omitted for clarity.

**Table IV.** Best fit kinetic parameters for NOB.

Parameter	Value
<i>Nitrobacter</i> spp.	
$\hat{\mu}_{\text{Nit}}$	0.31 day <sup>-1</sup>
$K_{\text{o,Nit}}$	0.51 g m <sup>-3</sup>
$K_{\text{s,Nit}}$	0.39 g N m <sup>-3</sup>
<i>Nitrospira</i> spp.	
$\hat{\mu}_{\text{Nsr}}$	0.28 day <sup>-1</sup>
$K_{\text{o,Nsr}}$	0.4 g m <sup>-3</sup>
$K_{\text{s,Nsr}}$	0.27 g N m <sup>-3</sup>

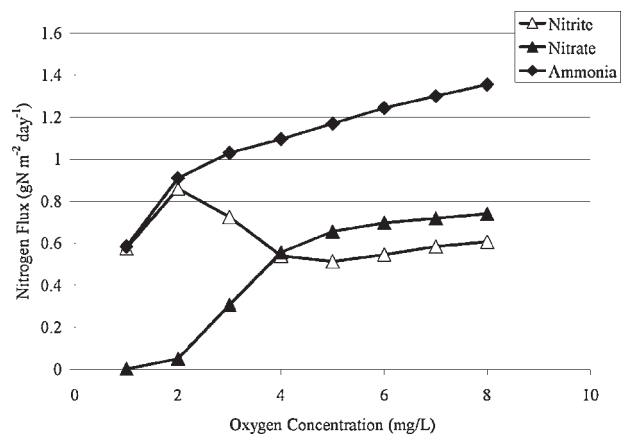
nitrite was dominant when the DO at the membrane surface was below 3 g m<sup>-3</sup>. The nitrite and nitrate fluxes were almost equal when the DO was 5 g m<sup>-3</sup>. Even at the high DO concentrations, a significant amount of nitrite accumulation was predicted (approximately 40%). This shows that considerable shortcut nitrogen removal is always present, an effect not captured by previous models that consider nitrification to nitrate in a single step (Shanahan and Semmens, 2004).

The impact of bulk liquid oxygen concentrations was also examined with the model. Experimental results indicated little difference in ammonium fluxes when the bulk liquid was anoxic (Experiment 3) or when the bulk DO was 2 g m<sup>-3</sup> (Experiment 4). The model predicted higher ammonium fluxes at higher bulk liquid DO concentrations, but generally lower percentages of nitrite accumulation (Table VI).

## Discussion

### Oxygen Gradients

The intra-membrane air supply pressure of an MAB is a readily controllable variable, and a desirable means for selecting for nitrite accumulation in the HMBP or other MAB systems. Microsensor measurements indicated that intra-membrane operating pressure effectively controlled the oxygen gradients in the MAB. Previous biofilm studies found an oxygen concentration of 2 g m<sup>-3</sup> to be an effective means for controlling nitrite accumulation in hybrid, suspended and attached-growth systems (Chung et al., 2007), and *Nitrobacter* spp. populations were shown to decrease in a nitrifying biofilm at around 2 g m<sup>-3</sup> (Schramm et al., 2000). In our studies, when the intra-membrane pressure was 35 kPa, the majority of the

**Figure 5.** Model-predicted fluxes of nitrite, nitrate, and ammonia at varying membrane surface DO concentrations.

biofilm had oxygen concentrations below 2 g m<sup>-3</sup>, and high levels of nitrite accumulation were observed. The entire biofilm was near or below 2 g m<sup>-3</sup> oxygen when the intra-membrane pressure was 14 kPa. While this low oxygen condition resulted in complete nitrite accumulation, reduced ammonium fluxes were observed.

### Nitrite Accumulation

Our results suggest that nitrite accumulation can be achieved in an MAB, even at high membrane-surface and bulk-liquid DO concentrations. In our experiments, the optimal condition occurred when the DO at the membrane surface was approximately 3.5 g m<sup>-3</sup> and the bulk liquid was anoxic (Experiment 2). In this case, almost complete nitrite accumulation was achieved, with relatively high ammonium oxidation fluxes. At lower membrane surface DO concentrations, the ammonium oxidation flux decreased significantly, while at higher DO concentrations, much less nitrite accumulation occurred. Modeling results indicated that nitrite accumulation exceeding 40% of the oxidized nitrogen can occur even at membrane DO concentrations of 8 g m<sup>-3</sup>. In practice, a compromise must be made between higher nitrification fluxes, leading to more compact treatment processes, and shortcut nitrification, leading to lower demands for electron donors for denitrification. The

**Table V.** Comparison of experimental and model fluxes for each experimental condition.

Experiment	Oxygen concentration (g m <sup>-3</sup> )	Flux					
		Ammonium (g N m <sup>-2</sup> day <sup>-1</sup> )		Nitrite (g N m <sup>-2</sup> day <sup>-1</sup> )		Nitrate (g N m <sup>-2</sup> day <sup>-1</sup> )	
		Exp.	Model	Exp.	Model	Exp.	Model
1	2.2	0.74	0.7	0.63	0.57	0.01	0.1
2	3.2	1.01	1.27	1	0.96	0.04	0.286
3	5.5	1.3	1.37	0.43	0.64	0.64	0.715
4	5.5	1.26	1.18	0.34	0.3	0.84	0.81

**Table VI.** Modeled fluxes for ammonium, nitrite, and nitrate as a function of DO at membrane interface and bulk liquid.

DO in bulk liquid (g m <sup>-3</sup> )	DO at membrane-biofilm interface											
	2 g m <sup>-3</sup>				4 g m <sup>-3</sup>				8 g m <sup>-3</sup>			
	NH <sub>4</sub> <sup>+</sup> (g N m <sup>-2</sup> day <sup>-1</sup> )	NO <sub>2</sub> <sup>-</sup> (g N m <sup>-2</sup> day <sup>-1</sup> )	NO <sub>3</sub> <sup>-</sup> (g N m <sup>-2</sup> day <sup>-1</sup> )	NO <sub>2</sub> <sup>-</sup> (%)	NH <sub>4</sub> <sup>+</sup> (g N m <sup>-2</sup> day <sup>-1</sup> )	NO <sub>2</sub> <sup>-</sup> (g N m <sup>-2</sup> day <sup>-1</sup> )	NO <sub>3</sub> <sup>-</sup> (g N m <sup>-2</sup> day <sup>-1</sup> )	NO <sub>2</sub> <sup>-</sup> (%)	NH <sub>4</sub> <sup>+</sup> (g N m <sup>-2</sup> day <sup>-1</sup> )	NO <sub>2</sub> <sup>-</sup> (g N m <sup>-2</sup> day <sup>-1</sup> )	NO <sub>3</sub> <sup>-</sup> (g N m <sup>-2</sup> day <sup>-1</sup> )	NO <sub>2</sub> <sup>-</sup> (%)
0	0.91	0.86	0.05	95	1.09	0.56	0.54	51	1.35	0.61	0.74	45
0.5	1	0.64	0.36	64	1.17	0.63	0.53	54	1.39	0.66	0.73	47
1	1.11	0.66	0.45	59	1.27	0.64	0.63	50	1.44	0.71	0.74	49
2	1.3	0.77	0.53	59	1.41	0.65	0.77	46	1.5	0.7	0.81	46

The percent nitrite column is the nitrate flux as a percent of the sum of nitrate and nitrate fluxes.

biofilm region with DO below 2 g m<sup>-3</sup> appears to control the extent of nitrite accumulation.

NOB cell densities decreased with decreasing DO concentrations, favoring nitrite accumulation. Also, the dominant species of NOB shifted from *Nitrobacter* spp. to *Nitrospira* spp. This is significant, because *Nitrospira* spp. have lower nitrite oxidation rates than *Nitrobacter* spp. (Table II). Even though NOB are present at low operating pressures, the slow kinetics of *Nitrospira* spp. results in reduced contribution to nitrate fluxes.

Kinetic parameters found through modeling indicated that the  $\hat{\mu}$  value for *Nitrobacter* spp. was higher than that for *Nitrospira* spp., whereas the K values for *Nitrospira* spp. were lower than *Nitrobacter* spp.. This is consistent with previous research suggesting that *Nitrobacter* spp. are r-strategists, whereas *Nitrospira* spp. are K-strategists (Blackburne et al., 2007b; Kim and Kim, 2006; Nogueira and Melo, 2006; Schramm et al., 1999). The best fit parameters indicate that *Nitrospira* spp. are favored in both low nitrite and low oxygen conditions. Previous research indicated nitrite to be the main factor governing competition between *Nitrobacter* spp. and *Nitrospira* spp. in suspended growth cultures (Blackburne et al., 2007b; Nogueira and Melo, 2006), whereas Schramm et al. (2000) found a *Nitrospira* spp. peak where oxygen disappeared in an MAB, suggesting that oxygen affinity may also play a role in selection of *Nitrospira* spp. over *Nitrobacter* spp. Our results suggest that both nitrite and oxygen affinity play a role in the selection of *Nitrospira* spp. over *Nitrobacter* spp, as the K for oxygen and nitrite for *Nitrospira* spp. is lower than for *Nitrobacter* spp. The lower  $\hat{\mu}$  value for *Nitrospira* spp. suggests that, even when *Nitrospira* spp. are present, they do not contribute to nitrate fluxes as much as *Nitrobacter* spp.

The shift in NOB population observed in the MABs would be expected to be similar in other biofilm systems where shortcut nitrification has been reported (e.g., biofilm airlift suspension (BAS) reactors (Garrido et al., 1996) and sponge based biofilm reactors (Chung et al., 2007)). A similar impact of oxygen concentration on nitrite accumulation would also be expected in biofilm systems with bulk aeration. The main difference between an MAB (where oxygen is delivered at the substratum) and a biofilm in a BAS or similar biofilm reactor (where oxygen is supplied via the bulk liquid) is the location of the *Nitrobacter* spp in the biofilm. In a biofilm with bulk-liquid aeration, the *Nitrobacter* spp. are located at the outer edge of the biofilm, where the oxygen concentration is the highest, whereas in the MAB the *Nitrobacter* spp are located at the base of the biofilm. Due to the location of *Nitrobacter* spp., greater *Nitrobacter* spp. detachment and washout may occur in a biofilm system with bulk aeration (Elenter et al., 2007).

## Conclusions

Shortcut nitrification was quantified in an MAB as a function of membrane and bulk DO concentrations. The extent of nitrite formation was related to the fraction of biofilm with DO below 2 g m<sup>-3</sup>. A tradeoff exists between

obtaining high ammonium oxidation fluxes at high membrane DO concentrations and obtaining high nitrite accumulation at low membrane DO concentrations. In carbon limited wastewaters, it may be beneficial to operate an HMBP or MABR at decreased intra-membrane pressures to maximize nitrite production, minimizing exogenous electron donor requirements. In a wastewater with sufficient carbon, higher intra-membrane pressures may be desirable to achieve higher nitrification rates, while still achieving a substantial degree of nitrite accumulation.

Funding for this research was provided by the Cooperative Institute for Coastal and Estuarine Environmental Technology (CICEET), with additional support from the National Science Foundation (NSF) via the Graduate Fellowship Program. We would also like to thank Andreas Schramm and Peter Stief (University of Århus, Denmark) for sharing their expertise in microsensor construction and Lutgarde Raskin (University of Michigan) for training in her FISH protocol.

## Appendix A

### Appendix AI. Kinetic rate expressions.

Process	Rate expression
Aerobic ammonium oxidation	$q_{\max, \text{AOB}} Y_{\text{AOB}} \frac{\text{NH}_4^+}{\text{NH}_4^+ + K_{\text{S, AOB}}} \frac{\text{O}_2}{\text{O}_2 + K_{\text{O, AOB}}} X_{\text{AOB}}$
Aerobic nitrite oxidation, <i>Nitrobacter</i> spp.	$q_{\max, \text{Nit}} Y_{\text{Nit}} \frac{\text{NO}_2}{\text{NO}_2 + K_{\text{S, Nit}}} \frac{\text{O}_2}{\text{O}_2 + K_{\text{O, Nit}}} X_{\text{Nit}}$
Aerobic nitrite oxidation, <i>Nitrospira</i> spp.	$q_{\max, \text{Nsr}} Y_{\text{Nsr}} \frac{\text{NO}_2}{\text{NO}_2 + K_{\text{S, Nsr}}} \frac{\text{O}_2}{\text{O}_2 + K_{\text{O, Nsr}}} X_{\text{Nsr}}$
Decay of AOB	$b_{\text{AOB}} X_{\text{AOB}}$
Decay of <i>Nitrobacter</i> spp.	$b_{\text{Nit}} X_{\text{Nit}}$
Decay of <i>Nitrospira</i> spp.	$b_{\text{Nsr}} X_{\text{Nsr}}$

### Appendix AII. Stoichiometric matrix.

	$\text{NH}_4^+ \text{-N}$	$\text{NO}_2^- \text{-N}$	$\text{NO}_3^- \text{-N}$	$\text{O}_2$	$X_{\text{AOB}}$	$X_{\text{Nit}}$	$X_{\text{Nsr}}$
Aerobic ammonium oxidation	$\frac{-1}{Y_{\text{AOB}}}$	$\frac{1}{Y_{\text{AOB}}}$	—	$\frac{-(3.42 - 1.42Y_{\text{AOB}})}{Y_{\text{AOB}}}$	1	—	—
Aerobic nitrite oxidation, <i>Nitrobacter</i> spp.	—	$\frac{-1}{Y_{\text{Nit}}}$	$\frac{1}{Y_{\text{Nit}}}$	$\frac{-(1.14 - 1.42Y_{\text{Nit}})}{Y_{\text{Nit}}}$	—	1	—
Aerobic nitrite oxidation, <i>Nitrospira</i> spp.	—	$\frac{-1}{Y_{\text{Nsr}}}$	$\frac{1}{Y_{\text{Nsr}}}$	$\frac{-(1.14 - 1.42Y_{\text{Nsr}})}{Y_{\text{Nsr}}}$	—	1	—
Decay of AOB	—	—	—	—	-1	—	—
Decay of <i>Nitrobacter</i> spp.	—	—	—	—	—	-1	—
Decay of <i>Nitrospira</i> spp.	—	—	—	—	—	—	-1

### Appendix AIII. Physical Parameters.

Parameter	Description	Value	References
$\rho$	Biofilm density	10 kg m <sup>-3</sup>	Rittmann and McCarty (2001)
$D_{\text{NH}_4^+ \text{-N}}$	Diffusivity of ammonium	1.5 × 10 <sup>-4</sup> m <sup>2</sup> day <sup>-1</sup>	Adapted from Schramm et al. (1999)
$D_{\text{NO}_2^- \text{-N}}$	Diffusivity of nitrite	1.4 × 10 <sup>-4</sup> m <sup>2</sup> day <sup>-1</sup>	Adapted from Schramm et al. (1999)
$D_{\text{NO}_3^- \text{-N}}$	Diffusivity of nitrate	1.4 × 10 <sup>-4</sup> m <sup>2</sup> day <sup>-1</sup>	Adapted from Schramm et al. (1999)
$D_{\text{O}_2}$	Diffusivity of oxygen	1.5 × 10 <sup>-4</sup> m <sup>2</sup> day <sup>-1</sup>	Adapted from Schramm et al. (1999)
LDL	Thickness of liquid diffusion layer	7 μm	Calculated for this study

### Appendix AIV. Sensitivity analysis of NOB kinetic parameters.

Parameter	Percent change			
	Nitrite flux (%)	Nitrate flux (%)	<i>Nitrobacter</i> spp. population (%)	<i>Nitrospira</i> spp. population (%)
$\mu_{\text{Nit}}$	-20 <sup>a</sup>	<b>40</b>	<b>57</b>	-38
$\mu_{\text{Nsr}}$	-10	<b>14</b>	-26	<b>106</b>
$K_{\text{O, Nit}}$	3	-9	-8	6
$K_{\text{O, Nsr}}$	1	-2	-2	-11
$K_{\text{S, Nit}}$	3	-9	-12	6
$K_{\text{S, Nsr}}$	1	-2	-2	-13

<sup>a</sup>Values in bold indicate percent changes >10% during sensitivity analysis.

## References

- Amann R, Krumholz L, Stahl D. 1990. Fluorescent-oligonucleotide probing of whole cells for determinative, phylogenetic, and environmental studies in microbiology. *J Bacteriol* 172:762–770.
- Anthonisen AC, Loehr RC, Prakasam TBS, Srinath EG. 1976. Inhibition of nitrification by ammonia and nitrous acid. *J Water Pollut Control Fed* 48(5):835–852.
- Blackburne R, Vadivelu V, Yuan Z, Keller J. 2007a. Determination of growth rate and yield of nitrifying bacteria by measuring carbon dioxide uptake rate. *Water Environ Res* 79(12):2437–2445.
- Blackburne R, Vadivelu V, Yuan Z, Keller J. 2007b. Kinetic characterisation of an enriched *Nitrospira* culture with comparison to *Nitrobacter*. *Water Res* 41:3033–3042.
- Burrell P, Keller J, Blackall LL. 1999. Characterisation of the bacterial consortium involved in nitrite oxidation in activated sludge. *Water Sci Technol* 39(6):45–52.
- Chung J, Bae W, Lee YW, Rittmann BE. 2007. Shortcut biological nitrogen removal in hybrid biofilm/suspended growth reactors. *Process Biochem* 42:320–328.
- Cole AC, Semmens MJ, LaPara TM. 2004. Stratification of activity and bacterial community structure in biofilms grown on membranes transferring oxygen. *Appl Environ Microbiol* 70(4):1982–1989.
- De Beer D, Sweerts J-PRA. 1989. Measurement of nitrate gradients with an ion-selective microelectrode. *Anal Chim Acta* 219:351–356.
- De Beer D, van den Heuvel JC. 1988. Response of ammonium-selective microelectrodes based on the neutral carrier nonactin. *Talanta* 35(9):728–730.
- De Beer D, Schramm A, Santegoeds C, Kuhl M. 1997. A Nitrite Microsensor for Profiling Environmental Biofilms. *Appl Environ Microbiol* 63(3):973–977.
- Downing L, Nerenberg R. 2007. Microbial ecology and performance of a hybrid membrane biofilm process for concurrent nitrification and denitrification. *Water Sci Technol* 55(8–9):355–362.
- Downing L, Nerenberg R. 2008. Total nitrogen removal in a hybrid, membrane-aerated activated sludge process. *Water Res*, DOI: 10.1016/j.watres.2008.06.006.
- Ehrich S, Behrens D, Lebedeva E, Ludwig W, Bock E. 1995. A new obligately chemolithoautotrophic, nitrite-oxidizing bacterium, *Nitrospira moscoviensis* sp. nov. and its phylogenetic relationship. *Arch Microbiol* 164(1):16–23.
- Elenter D, Milferstedt K, Zhang W, Hausner M, Morgenroth E. 2007. Influence of detachment on substrate removal and microbial ecology in a heterotrophic/autotrophic biofilm. *Water Res* 41:4657–4671.
- Garrido JM, van Benthum WAJ, van Loosdrecht MCM, Heijnen JJ. 1996. Influence of dissolved oxygen concentration on nitrite accumulation in a biofilm airlift suspension reactor. *Biotechnol Bioeng* 53(2):168–178.
- Geiseke A, De Beer D. 2004. Use of microelectrodes to measure in situ microbial activities in biofilms, sediments, and microbial mats. In: Kowalchuk G, de Bruijn F, Head I, Akkermans A, van Elsas J, editors. *Molecular microbial ecology manual*. 2nd edn. Heidelberg: Springer.
- Harms G, Layton AC, Dionisi HM, Gregory IR, Garrett VM, Hawkins SA, Robinson KG, Saylor GS. 2003. Real-time PCR quantification of nitrifying bacteria in a municipal wastewater treatment plant. *Environ Sci Technol* 37(2):343–351.
- Hellinga C, Schellen A, Mulder J, van Loosdrecht MCM, Heijnen JJ. 1998. The SHARON process: An innovative method for nitrogen removal from ammonium-rich wastewater. *Water Sci Technol* 37(9):135–142.
- Hibiya K, Terada A, Tsuneda S, Hirata A. 2003. Simultaneous nitrification and denitrification by controlling vertical and horizontal microenvironment in a membrane-aerated biofilm reactor. *J Biotechnol* 100(1):23–32.
- Juretschko S, Timmerman G, Schmid MC, Schleifer K-H, Pomeroy-Roser A, Koops H-P, Wagner M. 1998. Combined molecular and conventional analyses of nitrifying bacterium diversity in activated sludge: *Nitrosococcus mobilis* and *Nitrospira*-like bacteria as dominant populations. *Appl Environ Microbiol* 64(8):3042–3051.
- Kim DJ, Kim SH. 2006. Effect of nitrite concentration on the distribution and competition of nitrite-oxidizing bacteria in nitrification reactor systems and their kinetic characteristics. *Water Res* 40:887–894.
- Kindaichi T, Kawano Y, Ito T, Satoh H, Okabe S. 2006. Population dynamics and in situ kinetics of nitrifying bacteria in autotrophic nitrifying biofilms as determined by real-time quantitative PCR. *Biotechnol Bioeng* 94(6):1111–1121.
- Laanbroek HJ, Gerards S. 1993. Competition for limiting amounts of oxygen between *Nitrosomonas europaea* and *Nitrobacter winogradskyi* grown in mixed continuous culture. *Arch Microbiol* 159:453–459.
- Laanbroek HJ, Bodelier PLE, Gerards S. 1994. Oxygen consumption kinetics of *Nitrosomonas europaea* and *Nitrobacter hamburgensis* grown in mixed continuous cultures at different oxygen concentrations. *Arch Microbiol* 161:156–162.
- LaPara TM, Cole AC, Shanahan JW, Semmens MJ. 2006. The effects of organic carbon, ammoniacal-nitrogen, and oxygen partial pressure of the stratification of membrane-aerated biofilms. *J Ind Microbiol Biotechnol* 33(4):315–323.
- Manahan SE. 1993. *Fundamentals of environmental chemistry*. Chelsea, Michigan: Lewis Publishers.
- Manz W, Amann R, Ludwig W, Wagner M, Schleifer K-H. 1992. Phylogenetic oligodeoxynucleotide probes for the major subclasses of proteobacteria: Problems and solutions. *Syst Appl Microbiol* 15:593–600.
- Mobarry BK, Wagner M, Urbain V, Rittmann BE, Stahl DA. 1996. Phylogenetic probes for analyzing abundance and spatial organization of nitrifying bacteria. *Appl Environ Microbiol* 62(6):2156–2162.
- Munich EV, Lant P, Keller J. 1996. Simultaneous nitrification and denitrification in bench-scale sequencing batch reactors. *Water Res* 30(2):277–284.
- Nogueira R, Melo LF. 2006. Competition between *Nitrospira* spp. and *Nitrobacter* spp. in nitrite oxidizing bioreactors. *Biotechnol Bioeng* 95:169–175.
- Pochana K, Keller J. 1999. Study of factors affecting simultaneous nitrification and denitrification (SND). *Water Sci Technol* 39(6):61–68.
- Prosser JI. 1989. Autotrophic nitrification in bacteria. *Adv Microb Physiol* 30:125–181.
- Revsbech NP, Jørgensen BB. 1986. Microelectrodes: Their use in microbial ecology. *Adv Microb Ecol* 9:293–352.
- Rittmann BE, McCarty PL. 2001. *Environmental biotechnology: Principles and applications*. New York: McGraw-Hill.
- Satoh H, Okabe S, Watanabe Y. 2000. Significance of substrate C/N ratio on the structure and activity of nitrifying biofilms determined by in situ hybridization and the use of microelectrodes. *Water Sci Technol* 41(5):317–321.
- Schramm A, DeBeer D, Wagner M, Amann R. 1998. Identification and activities in situ of *Nitrosospira* and *Nitrospira* spp. as dominant populations in a nitrifying fluidized bed reactor. *Appl Environ Microbiol* 64(9):3480–3485.
- Schramm A, De Beer D, van den Heuvel JC, Ottengraf S, Amann R. 1999. Microscale distribution of populations and activities of *Nitrosospira* and *Nitrospira* spp. along a macroscale gradient in a nitrifying bioreactor: quantification by in situ hybridization and the use of micro-sensors. *Appl Environ Microbiol* 65(8):3690–3696.
- Schramm A, De Beer D, Gieseke A, Amann R. 2000. Microenvironments and distribution of nitrifying bacteria in a membrane-bound biofilm. *Environ Microbiol* 2(6):680–686.
- Semmens MJ, Dahm K, Shanahan J, Christianson A. 2003. COD and nitrogen removal by biofilms growing on gas permeable membranes. *Water Res* 37(18):4343–4350.
- Shanahan J, Semmens MJ. 2004. Multipopulation model of membrane-aerated biofilms. *Environ Sci Technol* 38(11):3176–3183.
- Shanahan J, Cole AC, Semmens MJ, LaPara TM. 2005. Acetate and ammonium diffusivity in membrane-aerated biofilms: Improving model predictions using experimental results. *Water Sci Technol* 52(7):121–126.

- Siripong S, Rittmann BE. 2007. Diversity study of nitrifying bacteria in full-scale municipal wastewater treatment plants. *Water Res* 41(5):1110–1120.
- Slikkers AO, Haaijer Suzanne CM, Stafsnes MH, Kuenen JG, Jetten MSM. 2005. Competition and coexistence of aerobic ammonium and nitrite-oxidizing bacteria at low oxygen concentrations. *Appl Microbiol Biotechnol* 68:808–817.
- Syron E, Casey E. 2008. Membrane-aerated biofilm for high rate biotreatment: Performance appraisal, engineering principles, scale-up, and development requirements. *Environ Sci Technol* 42(4):1833–1845.
- Terada A, Hibiya K, Nagai J, Tsuneda S, Hirata A. 2003. Nitrogen removal characteristics and biofilm analysis of a membrane-aerated biofilm reactor applicable to high-strength nitrogenous wastewater treatment. *J Biosci Bioeng* 95(2):170–178.
- Terada A, Yamamoto T, Igarashi R, Tsuneda S, Hirata A. 2006. Feasibility of a membrane-aerated biofilm reactor to achieve controllable nitrification. *Biochem Eng J* 28(2):123–130.
- Timberlake D, Strand S, Williamson K. 1988. Combined aerobic heterotrophic oxidation, nitrification and denitrification in a permeable-support biofilm. *Water Res* 22(12):1513–1517.
- van Loosdrecht MCM, Jetten MSM. 1998. Microbiological conversions in nitrogen removal. *Water Sci Technol* 38(1):1–7.
- Villaverde S, Garcia-Encina PA, Fernandez-Polanco F. 1997. Influence of pH over nitrifying biofilm activity in submerged biofilters. *Water Res* 31(5):1180–1186.
- Wagner M, Rath G, Koops HP, Flood J, Amann R. 1996. In situ analysis of nitrifying bacteria in sewage treatment plants. *Water Sci Technol* 34: 237–244.
- Walter B, Haase C, Rabiger N. 2005. Combined nitrification/denitrification in a membrane reactor. *Water Res* 39(13):2781–2788.
- Wanner O, Reichert P. 1996. Mathematical modeling of mixed-culture biofilms. *Biotechnol Bioeng* 49(2):172–184.
- Wiesmann U. 1997. Biological nitrogen removal from wastewater. In: Fiechter A, editor. *Advances in biochemical engineering/biotechnology*. Berlin: Springer-Verlag. p 113–154.
- Yang Q, Peng Y, Liu X, Zeng W, Takashi M, Satoh H. 2007. Nitrogen removal via nitrite from municipal wastewater at low temperatures using real-time control to optimize nitrifying communities. *Environ Sci Technol* 41(23):8159–8164.